



Assessment of spatial uncertainty of heavy local rainfall using a dense gauge network

Sungmin O^{1,2,*} and Ulrich Foelsche^{1,2,3}

¹Institute for Geophysics, Astrophysics, and Meteorology/Institute of Physics (IGAM/IP), NAWI Graz, University of Graz, Austria

²FWF-DK Climate Change, University of Graz, Austria

³Wegener Center for Climate and Global Change (WEGC), University of Graz, Austria

*Now at Biogeochemical Integration, Max Planck Institute for Biogeochemistry, Jena, Germany

Correspondence: Sungmin O (sungmin.o@uni-graz.at)

Abstract. Hydrology and remote-sensing communities have made use of dense rain-gauge networks for studying rainfall uncertainty and variability. However, in most regions, these dense networks are only available at sub-pixel scales and over short periods of time. Just a few studies have applied a similar approach, employing dense gauge networks, to local-scale areas, which limits the verification of their results in other regions. Using 10-year rainfall measurements from a network of 150 rain gauges, WegenerNet (WEGN), we assess spatial uncertainty in observed heavy rainfall events. The WEGN network is located in southeastern Austria over an area of 20 km × 15 km with moderate orography. First, the spatial variability of rainfall in the region was characterised using a correlogram at daily and sub-daily scales. Differences in the spatial structure of rainfall events between wet and dry seasons are apparent and we selected heavy rainfall events, the upper 10% of wettest days during the wet season, for further analyses because of their high potential for causing hazards. Secondly, we investigated the uncertainty in estimating mean areal rainfall arising from a limited gauge density. The number of gauges required to obtain areal rainfall with errors less than 20% tends to increase roughly following a power law as time scale decreases. Lastly, the impact of spatial aggregation on extreme rainfall was examined, using gridded rainfall data with horizontal grid spacings from 0.1° to 0.01°. The spatial scale dependence was clearly observed at high intensity thresholds and high temporal resolutions. Quantitative uncertainty information from this study can guide both data users and producers to estimate uncertainty in their own observational datasets, consequently leading to the sensible use of the data in relevant applications. Our findings are generalisable to moderately hilly region in mid-latitudes, however the degree of uncertainty could be affected by regional variations, like rainfall type or topography.

1 Introduction

Rainfall data are one of the most important inputs for hydrological as well as climatological studies and applications. Furthermore, fit-for-purpose information derived from rainfall data is crucial for a wider range of users, such as civil engineers, water resource managers and governments. To meet the needs of diverse user groups, rainfall observational datasets from in-situ measurement and remote sensing have been greatly enhanced in terms of both data quality and resolution (e.g., Berezowski



et al., 2016; Hou et al., 2014; Keller et al., 2015; Yatagai et al., 2012). Often, rainfall data are required as areal estimates at the scale of interest, for instance, at grid or catchment scales. Point measurements from in-situ gauge observations are spatially aggregated or interpolated to estimate the areal distribution of rainfall, and hence the accuracy of areal rainfall data is highly dependent on spatiotemporal variability of rainfall events and density of observation points (Girons Lopez et al., 2015; Hofstra et al., 2010; Villarini et al., 2008; Wood et al., 2000). This limits understanding of fine-scale rainfall processes, particularly of extreme events (Sillmann et al., 2017). Although relatively higher-resolution data from remotely sensed observations (e.g., radar provides rainfall estimates at scales of 1 km/5-min) address a number of the issues relating to the scarcity of gauges, still rainfall variability cannot be fully captured at the sub-pixel scale (Peleg et al., 2013; Tokay et al., 2014). In addition, the quality of remotely sensed data strongly relies on gauge-based data that are used for their regional validation and correction (Steiner et al., 1999).

Addressing the issue of spatial variability and uncertainty of rainfall has been tackled over many years with various purposes. For instance, evaluation of satellite or radar rainfall products involves investigation of small-scale rainfall processes to identify the effect of intra-pixel variability of rainfall on the performance of remote sensing. On the other hand, larger-scale rainfall processes are of interest to assess the ability of remote sensing in capturing the inter-pixel rainfall variability (e.g., Ciach and Krajewski, 1999, 2006; Gebremichael and Krajewski, 2004; Habib and Krajewski, 2002; Peleg et al., 2013; Tokay et al., 2014). To quantify the rainfall uncertainty, observational data from high-resolution rain-gauge networks have been employed as a ground truth. Peleg et al. (2013) used multiple rain gauges within a radar subpixel area (4 km²) and examined the contribution of gauge sampling error to the total radar-rainfall estimation error. Using relatively long-term gauge data (5-years), Tokay et al. (2014) analyzed the spatial correlation of rainfall for different seasons and weather systems within the footprint size of microwave satellite sensor.

A similar approach employing dense gauge networks can be adopted to diagnose the spatial variability and uncertainty of rainfall at local-scale areas (e.g., 100 - 500 km²). Such a scale is of great interest not only for the evaluation of remotely sensed data, but also for hydrological applications like runoff modelling or gauge network design. Wood et al. (2000) examined the accuracy of areal estimates of rainfall over a 135 km² basin according to the HYdrological Radar EXperiment network consisting of 49 rain gauges. The network later provided a six-year rainfall dataset (from 50 gauges) for the study of Villarini et al. (2008), where a comprehensive analysis of temporal and spatial sampling uncertainties was conducted. However, most of the local areas do not have adequately dense gauge networks, which limits the comparison and verification of findings from the aforementioned studies across diverse rainfall regimes.

In order to contribute to the effort for better assessing the uncertainty of rainfall at fine scales associated with the spatial variability of local rainfall, we employed 10-year rainfall data from WegenerNet Feldbach region (WEGN), a high-density network in southeastern Austria (Kirchengast et al., 2014). The network includes 150 rain gauges deployed over an area of \simeq 300 km², approximately corresponding to one gauge per 2 km². First, following previous studies (e.g., Villarini et al., 2008; Peleg et al., 2013; Tokay et al., 2014), we quantified the spatial variability of rainfall utilizing a corrollogram between the gauges to understand the spatial characteristics of rainfall in the region.

Second, we investigated uncertainty in estimating areal rainfall based on a limited number of point observations. Given that



the properties of individual rainfall events can be different from all-event averages (Ciach and Krajewski, 2006; Eggert et al., 2015), we focused on potentially high-impact events, which we defined as the top 10% wettest days during the wet season. The accuracy of areal rainfall estimation is a long-standing issue, e.g., in catchment modelling because error and uncertainty in rainfall data can propagate into large variations in simulated runoff, and thus it has been dealt with in diverse manners. For instance, the influence of spatial representations of rainfall input to runoff errors has been demonstrated through modelling studies (e.g., Bárdossy and Das, 2008; Xu et al., 2013) or the error in catchment-scale areal mean rainfall has been directly quantified by employing high-resolution gauge data (e.g., Wood et al., 2000; Villarini et al., 2008; Ly et al., 2011).

Finally, we assessed the impact of spatial averaging on extreme rainfall using gridded rainfall fields. The identification of rainfall extremes based on intensity thresholds is common practice, however, the considered spatial scale of rainfall data defines different sets of extreme events (Eggert et al., 2015), potentially affecting threshold-based early warning systems (Marra et al., 2017). Although gridded datasets have been used in a range of applications like assessments of climate change impacts or evaluation of climate models, a common caveat of using the datasets in the study of extreme rainfall is that the quality of gridded rainfall data is highly constrained by the location and density of input weather station data (Hofstra et al., 2010; Prein and Gobiet, 2017). By contrast, the quasi-regular configuration of WEGN on an approximately 1.4 km x 1.4 km grid permits robust examination of the frequency and intensity of rainfall extremes at various horizontal resolutions.

Consequently, this study aims to assess spatial uncertainty of local-scale rainfall using rain gauge data, with a focus on heavy and extreme rainfall events. This paper is structured as follows. Section 2 describes WEGN rain gauge data and regional rainfall climatology. Section 3 to Sect. 5 present the results of the data analysis. We close with discussion and conclusions in Sect. 6.

20 2 WEGN rainfall data and regional rainfall climatology

The 10-year rainfall data (2007-2016) are obtained from the WEGN Feldbach region network in southeastern Austria (Kirchengast et al., 2014). Of 154 weather stations, 150 stations that are equipped with tipping-bucket rain gauges are used in this study (Fig. 1). The gauges record rainfall every five minutes. Errors in the rainfall data were comprehensively analysed and corrected by O et al. (2018). The gauges are uniformly spaced over an area of 20 km × 15 km with moderate topography. The inter-gauge distances range from approximately 0.7 km to 23.4 km. The gridded fields of rainfall are constructed by an inverse distance weighting (IDW) on a 200 m × 200 m Universal Transverse Mercator grid. WEGN station and gridded data products are available at www.wegenet.net.

Southeastern Austria including the Feldbach region is influenced by both continental and Mediterranean climates. The region receives high amounts of rainfall during summer months. The occurrence of thunderstorms and hail is higher than in other parts of Austria (Matulla et al., 2003). Figure 2 shows average diurnal variations of rainfall and temperature over the entire network during the study period. The WEGN area is characterized by hot and wet months from May through September (hereafter “wet season”) and relatively cold months without much rainfall during the remaining seven months (hereafter “dry season”). The average monthly rainfall is 102.8 mm in the wet season, while 48.9 mm in the dry season. The diurnal signal is more clearly



seen in the wet season for both rainfall and temperature. Rainfall maxima occur in the early afternoon through midnight, shortly after maximum temperature, implying that a major contribution to the wet season rainfall is from short-duration convective events. Because diurnal heating plays an important role in triggering thermal convection, most inland regions show afternoon rainfall maxima (Dai et al., 2007).

5 3 Spatial variability of rainfall

The spatial structure of rainfall events is studied using the Pearson's correlation coefficient (Villarini et al., 2008; Peleg et al., 2013; Tokay et al., 2014). At sub-daily and daily timescales from 5-min to 24-h (06-06 UTC), the correlation of rainfall among rain gauges is calculated for each year. One year period includes a set of wet season (May to September) and dry season (October to next April). The incomplete years (i.e., first and last years) are excluded from the calculation of all-months
10 (May to next April), whereas the wet and dry seasons have 10 annual curves each. Figure 3 shows the spatial correlation of all-months, wet, and dry seasons for four selected accumulation times. Following Villarini et al. (2008), we fitted a three-parameter exponential function to the observed correlations. The spatial correlation (r) at separation distance h is:

$$r(h) = c_1 \exp \left[- \left(\frac{h}{c_2} \right)^{c_3} \right] \quad (1)$$

where c_1 is the nugget, c_2 is the correlation distance, and c_3 is the shape factor. To reduce bias in the Pearson's estimates due
15 to non-normality of rainfall, a logarithmic transformation is applied to the data (Habib et al., 2001; Jaffrain and Berne, 2012). The function parameters tend to be sensitive to factors like rainfall type or sample size and thus we do not make a direct comparison with other studies in terms of absolute values. Nevertheless, the functions found in this study show a broad agreement with those from previous studies. First, longer accumulation times show higher zero-distance correlation (nugget) and longer correlation distance values. Second, short-range correlation decreases rapidly with increasing separation distance, particularly
20 at sub-hourly scales.

The wet season shows higher spatial variability of rainfall compared to the dry season, due to a higher proportion of convective events. The correlation curves of all-months show a more similar pattern with the wet season, as expected, given that most of the rainfall events are concentrated during the wet season (see Sect. 2). Tokay et al. (2014) found substantial year-to-year variations especially during autumn and spring. Similarly, WEGN rainfall shows marked interannual variability, but also during
25 the wet season. It should be noted that the correlation functions of the dry season start with lower nugget values than of the wet season. The nugget implies measurement errors and microscale variability of rainfall. Because WEGN does not accurately capture solid precipitation (O et al., 2018), since only few gauges are heated, systematic errors between neighboring gauges can be greater during the dry season, possibly yielding the low nugget values.

Figure 4 summarizes the time dependence of the three parameters. Nugget values range from 0.73 to 0.98 for the dry season,
30 while from 0.89 to 1.00 for the wet season. The correlation distance of the dry season is stretched up to around 200 km at the 6-h scale, while the same distance is observed at the 24-h scale in the wet season. The parameter values of all-months are located between those of wet season and dry season. We found that the general behaviour of nugget and correlation distance



is similar to Villarini et al. (2008). The shape factor of this study, however, does not show a uniform increasing or decreasing trend. This is consistent with findings from Peleg et al. (2013) and Tokay et al. (2014).

4 Accuracy of areal rainfall estimation during heavy rainfall events

In this section we investigate data uncertainty associated with areal rainfall estimation. In particular, the study focuses on high-impact rainfall events. While heavy rainfall is one of the major hydrological hazards, its accurate spatial representation over an area remains a subject worthy of inquiry. Based on daily rainfall ($\geq 0.2 \text{ mm d}^{-1}$), those days falling in the upper 10th percentile during the wet season are defined as heavy rainfall events. As a result, a total of 71 events are selected. The mean of gauge-averaged accumulations is 31.5 mm d^{-1} , with a range of 19.8 mm d^{-1} to 64.1 mm d^{-1} .

We assume that the mean areal rainfall of a full density network represents the “truth” (see also Villarini et al., 2008). The areal rainfall of n -gauge networks (n = number of gauges) is calculated with 1,000 possible combinations and then compared with the true rainfall. The 1-gauge network has 150 cases. As shown in Fig. 5a, the average and spread of normalized root-mean-square errors (NRMSEs) of areal rainfall estimated from low-density networks tend to decrease with rising gauge number. The number of gauges required to obtain areal rainfall with NRMSEs lower than 20% is given as a function of time resolution in Fig. 5b. The curve roughly exhibits power-law behavior; $74.19 \times t^{-0.44}$, where t is the time resolution. At the daily scale, more than one gauge per 300 km^2 would be sufficient to reach the $>20\%$ accuracy level. Correspondingly, at the temporal scales of 1-h, 30-min, and 5-min, more than 12, 18, and 33 gauges, respectively, are needed to achieve the same level of accuracy. Villarini et al. (2008) found that four gauges are necessary at the daily scale for the same accuracy level for an area of 135 km^2 . Heavy events are not explicitly considered in their study.

Additionally, the effect of gauge density on event-based rainfall statistics is assessed in Fig. 6. Daily rainfall accumulation and peak hourly rainfall of the 71 heavy daily events are recalculated using predefined sub-networks with gauges ranging from 1 to 16. The definition of the sub-networks can be found in Appendix A. While the sub-network with only one gauge exhibits large overestimation errors for both total and peak rainfall, employing an additional gauge already significantly reduces the degree of errors and yields underestimation error more frequently than overestimation. Note that Austrian weather service (ZAMG) has two operational stations over the actual WEGN area. Given that convective storms occur on scales of a few kilometers, low-density gauges over the region are likely to miss the core of storms. On the contrary, low-density gauges often overestimate rainfall intensities by capturing only the core of storms, but the magnitude and frequency of the errors appear slightly less than those of the underestimation error. There is no significant difference in either average error or spread of errors from more than 10 gauges, as expected from Fig. 5.

5 Impact of spatial scaling on extreme rainfall

We next focus on the uncertainty of area- or grid-averaged rainfall relating to data spatial resolution. Figure 7 compares rainfall percentiles among the gauges. Grey lines mean a 10-90th percentile range of rainfall intensities at a given percentile bin. For



example, at the 30-min scale, the 99.9th percentile (the top 0.1%) rainfall intensity corresponds to roughly 45 mm d^{-1} at most gauges, while it exceeds 52 mm d^{-1} at certain gauges. It is also seen that 10% of WEGN gauges (i.e., 15 gauges) records are found to be lower than 40 mm d^{-1} . The upper tail of rainfall distribution shows strong spatial variation. Such point-scale extreme rainfall features will be completely missed unless there exist dense rainfall observations, or they are inherently smoothed out in gridded data.

In fact, many studies have pointed out that the use of gridded rainfall data can lead to erroneous analyses of small-scale extremes because of the limited number of point observations (Hofstra et al., 2010; Tozer et al., 2012; Contractor et al., 2015; Prein and Gobiet, 2017). In addition to the high-resolution, the regular distribution of WEGN gauges enables generating gridded rainfall fields that are homogeneous in space, and, consequently, robustly assessing uncertainty in rare and extreme rainfall represented in the data.

We generated gridded data at horizontal resolutions from 0.01 to 0.1 degree (hereafter HR01 to HR10). Spatial aggregation begins from the top-left corner towards the bottom right and the remaining southern and/or eastern part of grid is discarded (see Fig 9). HR01 corresponds to about 1.1 km and 0.8 km in latitudinal and longitudinal directions, respectively. Figure 8 shows the 99.9th and 99th percentiles of heavy rainfall intensities as a function of space-time scales. HR01 clearly portrays the benefit of using dense networks to capture fine-scale extreme values, however spatial aggregation brings about the smoothing of rainfall intensities, notably at the sub-hourly scales. The decrease in 5-min rainfall intensity from HR01 to HR10 is 30% for the 99.9th percentile while it is 20% for the 99th percentile.

Meanwhile, the spatial scaling impact is much less pronounced at a daily scale, where the selected spatial scale still affects statistics of extreme areal rainfall, such as daily extreme frequency. This is shown in Fig. 9, which illustrates the occurrence of days above a selected threshold; top 5% of heavy rainfall events at HR01. The concept of the exceedance probability above thresholds is widely used in analyses of rainfall-triggered risk. Several HR01 sites have experienced extreme rainfall more frequently than others. In other words, high-resolution data well-represent spatial variation and frequency of rainfall extremes, neither of which is seen in lower-resolution data. Many existing gridded datasets are not likely to fully sample such site-level extreme events owing to their spatial scales being limited by sparse observation used to produce the dataset. The exceedance probability of extreme rainfall across spatial resolutions is given in Fig. 10. The impact of different resolutions on extreme rainfall occurrence is pronounced in the lower and upper tails. The 10-year rainfall maximum appears to be 68.4 mm/day at HR10, but 104.4 mm/day at HR01. Over the entire WEGN area, the maximum record is 64.1 mm/day ; +7% to +63% of increases in extreme rainfall intensities are observed depending on the considered spatial scale.

6 Discussion and conclusions

The understanding of spatial uncertainty in local heavy rainfall at fine scales has been hampered by the limited availability of suitable and reliable observational datasets. Although high-resolution radar data are often used to study small-scale rainfall variability, the use of the radar data is dubious, as indicated by Svensson and Jones (2010), owing to their indirect measurements of rain and relatively short records. In this study, we used the 10-year rainfall measurement data from the 150 rain



gauges, uniformly spaced over the WEGN network in southeastern Austria. First, to quantify rainfall variability, spatial correlation between the gauge records is examined. We found that the degree of rainfall spatial variability can be substantially different not only within years (wet versus dry seasons) but also between years. This implies that long-term data should be considered in this light to obtain comprehensive perspectives on regional rainfall variability. In fact, individual weather systems can exhibit varied spatial characteristics (Habib and Krajewski, 2002; Ciach and Krajewski, 2006; Tokay et al., 2014). In southeastern Austria, including the WEGN area, Schroeer et al. (2018) found much steeper decay in a correlogram function when only extreme summertime convective events are accounted for. Additionally, we found that during the dry season, the density of gauges is less of a concern (i.e., longer correlation distance) compared to the wet season. However, low values of zero-distance correlation imply that snow measurement during winter time remains a challenge, especially at short time scales.

Secondly, we confirm that the 150 gauges of WEGN offer very highly accurate areal precipitation estimates. The uncertainty in mean areal rainfall shows there to be a high dependence on the number of gauges and the temporal resolution considered for the estimation. Seeing that only two operational meteorological stations exist over the WEGN area, the accuracy of areal rainfall data obtained under normal circumstances could be inadequate for particular purposes, especially at sub-daily scales. We also investigated the effect of gauge density on total amount and peak hourly intensity of the daily heavy rainfall events. In the WEGN area (300 km²), it is observed that at least 2-5 gauges are required for areal rainfall estimates such that we can obtain reliable rainfall event statistics with no significant error. More than 5 gauges guarantee a high accuracy of the areal rainfall estimates. Our findings have implications concerning the use of sparse gauge observational data, for instance, in hydrologic modeling or rainfall estimates evaluation (e.g., Syed et al., 2003; Tian et al., 2018).

Lastly, using gridded WEGN data, rainfall extremes are reproduced at multiple spatial scales; approximately from the grid resolution of regional to convective-permitting models (about 11.1 km to 1.1 km in latitudinal direction). The results demonstrate that high-resolution gridded data provide more reliable information not only in terms of the magnitude and frequency of extremes, but also in terms of the exact location of the extremes. As a result, the limited spatial scale of rainfall data can alter interpretations of rainfall statistics; extreme rainfall events at a location of interest (a 0.01° × 0.01° site in our example) could occur more frequently and more intensely versus the local average. Localized information from high-resolution observation is the key to developing prevention and protection plans to mitigate potential damages of extreme rainfall in an efficient and adequate way. Our results highlight the need to evaluate uncertainty in extreme statistics derived from the existing datasets for supporting data selection among available rainfall data products.

In conclusion, the WEGN network provides a unique opportunity to empirically assess spatial variability and uncertainty of surface rainfall directly based on gauge data. The network provides long-term records, of more than a decade, which enable obtaining statistically robust results. Nonetheless, as stated in Villarini et al. (2008), there are only a few dense gauge networks on the local scale, so the verification of findings from studies in other regions is challenging. Regional variations, such as topography, can lead to differences in the degree of rainfall variability and uncertainty (e.g., Buytaert et al., 2006; Prein and Gobiet, 2017). Therefore, the general conclusions of this study should only be generalized for mid-latitude regions with moderate topography. It should be noted that WEGN has a high flexibility in terms of providing rainfall data within various



spatial scales thanks to both high-resolution and quasi-grid configuration of the gauges. In this context, WEGN will continue providing observational evidence to explore small-to-local scale rainfall processes over the next years.

Data availability. WegenerNet data products are available at www.wegenernet.org.

Appendix A: Definition of rain-gauge sub-networks

5 Figure A1 shows the selection order of WEGN gauges for defining the low-density sub-networks that were used in Fig. 6 of Sect. 4. Priority consideration was given to the actual location of operational weather stations within the WEGN network; the selected gauges 1 and 2 are located nearest to the member stations of the Austrian weather service (ZAMG) and the gauges 3, 4, and 5 are nearest to the rain gauges operated by the Austrian hydrographic services (AHYD). The gauges afterward were arbitrarily selected, ensuring a spatially uniform distribution. Normalized standard deviation of area-of-influence was used as
10 an index for the uniformity of gauge configuration, which fluctuated between 0.37 and 0.23 with a decreasing trend as the number of the selected gauges increases. The area-of-influence is defined as follows: small grid boxes (approx. $0.01^\circ \times 0.01^\circ$, a total of 406 boxes) were defined over the WEGN network and each box is assigned to the nearest gauges of a given sub-network. Then, with an assumption that the most regular gauge configuration would share the same number of boxes, standard deviation of the area-of-influence of n -gauges is calculated. For instance, for the *five-gauges* sub-network, each gauge is
15 expected to share around 80 boxes under an ideal situation. However, in this study, the five gauges share 71 to 113 boxes each, resulting in the uniformity index of 0.35. Note that this simple method does not consider the degree of centralization.

Competing interests. The authors declare that they have no conflict of interest.

Acknowledgements. The authors thank Prof. Kirchengast and J. Fuchsberger (University of Graz) for fruitful discussions. The study was fully funded by the Austrian Science Fund (FWF) under research grant W 1256-G15 (Doctoral Programme Climate Change Uncertainties,
20 Thresholds and Coping Strategies). WegenerNet funding is provided by the Austrian Ministry for Science and Research, the University of Graz, the state of Styria (which also included European Union regional development funds), and city of Graz.



References

- Bárdossy, A. and Das, T.: Influence of rainfall observation network on model calibration and application, *Hydrol. Earth Syst. Sci.*, 12, 77–89, <https://doi.org/10.5194/hess-12-77-2008>, 2008.
- Berezowski, T., Szcześniak, M., Kardel, I., Michałowski, R., Okruszko, T., Mezghani, A., and Piniewski, M.: CPLFD-GDPT5: High-resolution gridded daily precipitation and temperature data set for two largest Polish river basins, *Earth Syst. Sci. Data*, 8, 127–139, <https://doi.org/10.5194/essd-8-127-2016>, 2016.
- Buytaert, W., Celleri, R., Willems, P., Biévre, B. D., and Wyseure, G.: Spatial and temporal rainfall variability in mountainous areas: A case study from the south Ecuadorian Andes, *J. Hydrol.*, 329, 413–421, <https://doi.org/10.1016/j.jhydrol.2006.02.031>, 2006.
- Ciach, G. J. and Krajewski, W. F.: On the estimation of radar rainfall error variance, *Adv. Water Resour.*, 22, 585–595, [https://doi.org/10.1016/S0309-1708\(98\)00043-8](https://doi.org/10.1016/S0309-1708(98)00043-8), 1999.
- Ciach, G. J. and Krajewski, W. F.: Analysis and modeling of spatial correlation structure in small-scale rainfall in Central Oklahoma, *Adv. Water Resour.*, 29, 1450–1463, <https://doi.org/10.1016/j.advwatres.2005.11.003>, 2006.
- Contractor, S., Alexander, L. V., Donat, M. G., and Herold, N.: How well do gridded datasets of observed daily precipitation compare over Australia?, *Adv. Meteorol.*, 2015, 1–15, <https://doi.org/10.1155/2015/325718>, 2015.
- 15 Dai, A., Lin, X., and Hsu, K.-L.: The frequency, intensity, and diurnal cycle of precipitation in surface and satellite observations over low- and mid-latitudes, *Clim. Dyn.*, 29, 727–744, <https://doi.org/10.1007/s00382-007-0260-y>, 2007.
- Eggert, B., Berg, P., Haerter, J. O., Jacob, D., and Moseley, C.: Temporal and spatial scaling impacts on extreme precipitation, *Atmos. Chem. Phys.*, 15, 5957–5971, <https://doi.org/10.5194/acp-15-5957-2015>, 2015.
- Gebremichael, M. and Krajewski, W. F.: Assessment of the statistical characterization of small-scale rainfall variability from radar: analysis of TRMM ground validation datasets, *J. Appl. Meteorol. Clim.*, 43, 1180–1199, 2004.
- 20 Girons Lopez, M., Wennerström, H., Nordén, L.-Å., and Seibert, J.: Location and density of rain gauges for the estimation of spatial varying precipitation, *Geogr. Ann.: Ser. A, Phys. Geogr.*, 97, 167–179, <https://doi.org/10.1111/geoa.12094>, 2015.
- Habib, E. and Krajewski, W. F.: Uncertainty analysis of the TRMM ground-validation radar-rainfall products: Application to the TEFLUN-B field campaign, *J. Appl. Meteorol. Clim.*, 41, 558–572, [https://doi.org/10.1175/1520-0450\(2002\)041<0558:UAOTTG>2.0.CO;2](https://doi.org/10.1175/1520-0450(2002)041<0558:UAOTTG>2.0.CO;2), 2002.
- 25 Habib, E., Krajewski, W. F., and Ciach, G. J.: Estimation of rainfall interstation correlation, *J. Hydrometeorol.*, 2, 621–629, [https://doi.org/10.1175/1525-7541\(2001\)002<0621:EORIC>2.0.CO;2](https://doi.org/10.1175/1525-7541(2001)002<0621:EORIC>2.0.CO;2), 2001.
- Hofstra, N., New, M., and McSweeney, C.: The influence of interpolation and station network density on the distributions and trends of climate variables in gridded daily data, *Clim. Dyn.*, 35, 841–858, <https://doi.org/10.1007/s00382-009-0698-1>, 2010.
- Hou, A. Y., Kakar, R. K., Neeck, S., Azarbarzin, A. A., Kummerow, C. D., Kojima, M., Oki, R., Nakamura, K., and Iguchi, T.: The Global Precipitation Measurement mission, *Bull Am Meteorol Soc.*, 95, 701–722, <https://doi.org/10.1175/BAMS-D-13-00164.1>, 2014.
- Jaffrain, J. and Berne, A.: Quantification of the small-scale spatial structure of the raindrop size distribution from a network of disdrometers, *J. Appl. Meteorol. Clim.*, 51, 941–953, <https://doi.org/10.1175/JAMC-D-11-0136.1>, 2012.
- Keller, V. D. J., Tanguy, M., Prodocimi, I., Terry, J. A., Hitt, O., Cole, S. J., Fry, M., Morris, D. G., and Dixon, H.: CEH-GEAR: 1 km resolution daily and monthly areal rainfall estimates for the UK for hydrological and other applications, *Earth Syst. Sci. Data*, 7, 143–155, <https://doi.org/10.5194/essd-7-143-2015>, 2015.
- 35 Kirchengast, G., Kabas, T., Leuprecht, A., Bichler, C., and Truhetz, H.: WegenerNet: A pioneering high-resolution network for monitoring weather and climate, *Bull. Amer. Meteor. Soc.*, 95, 227–242, <https://doi.org/10.1175/BAMS-D-11-00161.1>, 2014.



- Ly, S., Charles, C., and Degré, A.: Geostatistical interpolation of daily rainfall at catchment scale: The use of several variogram models in the Ourthe and Ambleve catchments, Belgium, *Hydrol. Earth Syst. Sci.*, 15, 2259–2274, <https://doi.org/10.5194/hess-15-2259-2011>, 2011.
- Marra, F., Destro, E., Nikolopoulos, E. I., Zoccatelli, D., Creutin, J. D., Guzzetti, F., and Borga, M.: Impact of rainfall spatial aggregation on the identification of debris flow occurrence thresholds, *Hydrol. Earth Syst. Sci.*, 21, 4525–4532, <https://doi.org/10.5194/hess-21-4525-2017>, 2017.
- Matulla, C., Penlap, E. K., Haas, P., and Formayer, H.: Comparative analysis of spatial and seasonal variability: Austrian precipitation during the 20th century, *Int. J. Climatol.*, 23, 1577–1588, <https://doi.org/10.1002/joc.960>, 2003.
- O, S., Foelsche, U., Kirchengast, G., and Fuchsberger, J.: Validation and correction of rainfall data from the WegenerNet high density network in southeast Austria, *J. Hydrol.*, 556, 1110–1122, <https://doi.org/10.1016/j.jhydrol.2016.11.049>, 2018.
- 10 Peleg, N., Ben-Asher, M., and Morin, E.: Radar subpixel-scale rainfall variability and uncertainty: Lessons learned from observations of a dense rain-gauge network, *Hydrol. Earth Syst. Sci.*, 17, 2195–2208, <https://doi.org/10.5194/hess-17-2195-2013>, 2013.
- Prein, A. F. and Gobiet, A.: Impacts of uncertainties in European gridded precipitation observations on regional climate analysis: Uncertainty in European Precipitation, *Int. J. Climatol.*, 37, 305–327, <https://doi.org/10.1002/joc.4706>, 2017.
- Schroer, K., Kirchengast, G., and O, S.: Strong dependence of extreme convective precipitation intensities on gauge network density, *Geophys. Res. Lett.*, <https://doi.org/10.1029/2018GL077994>, accepted, 2018.
- 15 Sillmann, J., Thorarindottir, T., Keenlyside, N., Schaller, N., Alexander, L. V., Hegerl, G., Seneviratne, S. I., Vautard, R., Zhang, X., and Zwiers, F. W.: Understanding, modeling and predicting weather and climate extremes: Challenges and opportunities, *Weather. Clim. Soc.*, 18, 65–74, <https://doi.org/10.1016/j.wace.2017.10.003>, 2017.
- Steiner, M., Smith, J. A., Burges, S. J., Alonso, C. V., and Darden, R. W.: Effect of bias adjustment and rain gauge data quality control on radar rainfall estimation, *Water Resour. Res.*, 35, 2487–2503, <https://doi.org/10.1029/1999WR900142>, 1999.
- 20 Svensson, C. and Jones, D.: Review of methods for deriving areal reduction factors: Review of ARF methods, *J. Flood Risk Manag.*, 3, 232–245, <https://doi.org/10.1111/j.1753-318X.2010.01075.x>, 2010.
- Syed, K. H., Goodrich, D. C., Myers, D. E., and Sorooshian, S.: Spatial characteristics of thunderstorm rainfall fields and their relation to runoff, *J. Hydrol.*, 271, 1–21, [https://doi.org/10.1016/S0022-1694\(02\)00311-6](https://doi.org/10.1016/S0022-1694(02)00311-6), 2003.
- 25 Tian, F., Hou, S., Yang, L., Hu, H., and Hou, A.: How does the evaluation of the GPM IMERG rainfall product depend on gauge density and rainfall intensity?, *J. Hydrometeorol.*, 19, 339–349, <https://doi.org/10.1175/JHM-D-17-0161.1>, 2018.
- Tokay, A., Roche, R. J., and Bashor, P. G.: An experimental study of spatial variability of rainfall, *J. Hydrometeorol.*, 15, 801–812, <https://doi.org/10.1175/JHM-D-13-031.1>, 2014.
- Tozer, C. R., Kiem, A. S., and Verdon-Kidd, D. C.: On the uncertainties associated with using gridded rainfall data as a proxy for observed, *Hydrol. Earth Syst. Sci.*, 16, 1481–1499, <https://doi.org/10.5194/hess-16-1481-2012>, 2012.
- 30 Villarini, G., Mandapaka, P. V., Krajewski, W. F., and Moore, R. J.: Rainfall and sampling uncertainties: A rain gauge perspective, *J. Geophys. Res.*, 113, <https://doi.org/10.1029/2007JD009214>, 2008.
- Wood, S. J., Jones, D. A., and Moore, R. J.: Accuracy of rainfall measurement for scales of hydrological interest, *Hydrol. Earth Syst. Sci.*, 4, 531–543, <https://doi.org/10.5194/hess-4-531-2000>, 2000.
- 35 Xu, H., Xu, C.-Y., Chen, H., Zhang, Z., and Li, L.: Assessing the influence of rain gauge density and distribution on hydrological model performance in a humid region of China, *J. Hydrol.*, 505, 1–12, <https://doi.org/10.1016/j.jhydrol.2013.09.004>, 2013.



Yatagai, A., Kamiguchi, K., Arakawa, O., Hamada, A., Yasutomi, N., and Kitoh, A.: APHRODITE: Constructing a long-term daily gridded precipitation dataset for Asia based on a dense network of rain gauges, *Bull Am Meteorol Soc.*, 93, 1401–1415, <https://doi.org/10.1175/BAMS-D-11-00122.1>, 2012.

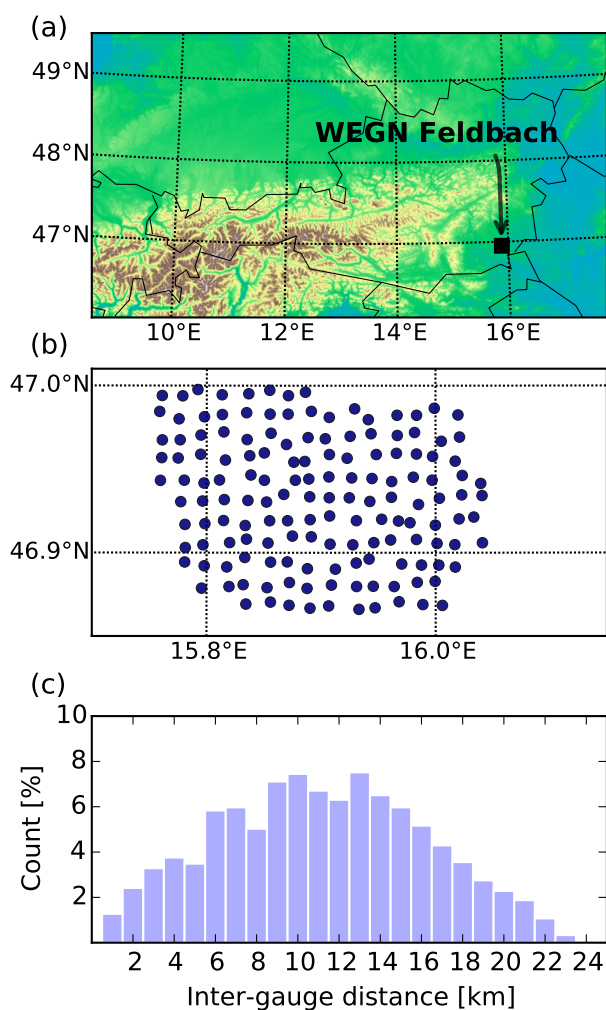


Figure 1. (a) WegenerNet Feldbach region (WEGN) network in southeastern Austria, (b) location of 150 tipping-bucket rain gauges, and (c) inter-gauge distances, rounded to the nearest 1-km bins.

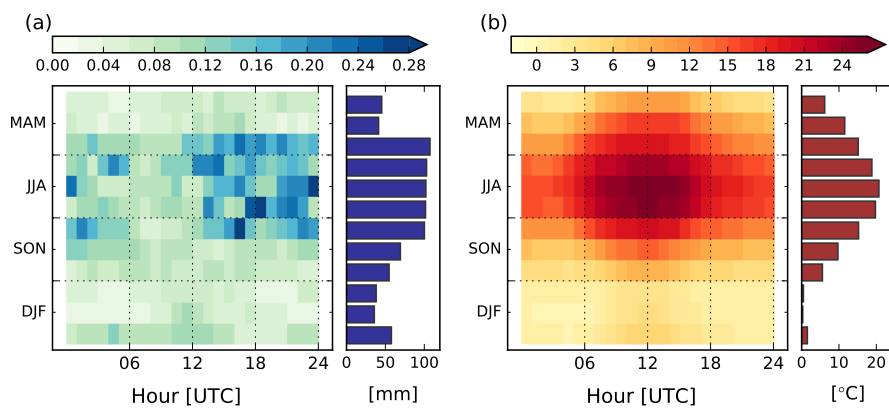


Figure 2. Diurnal cycles of (a) rainfall and (b) temperature derived from WEGN observational data.

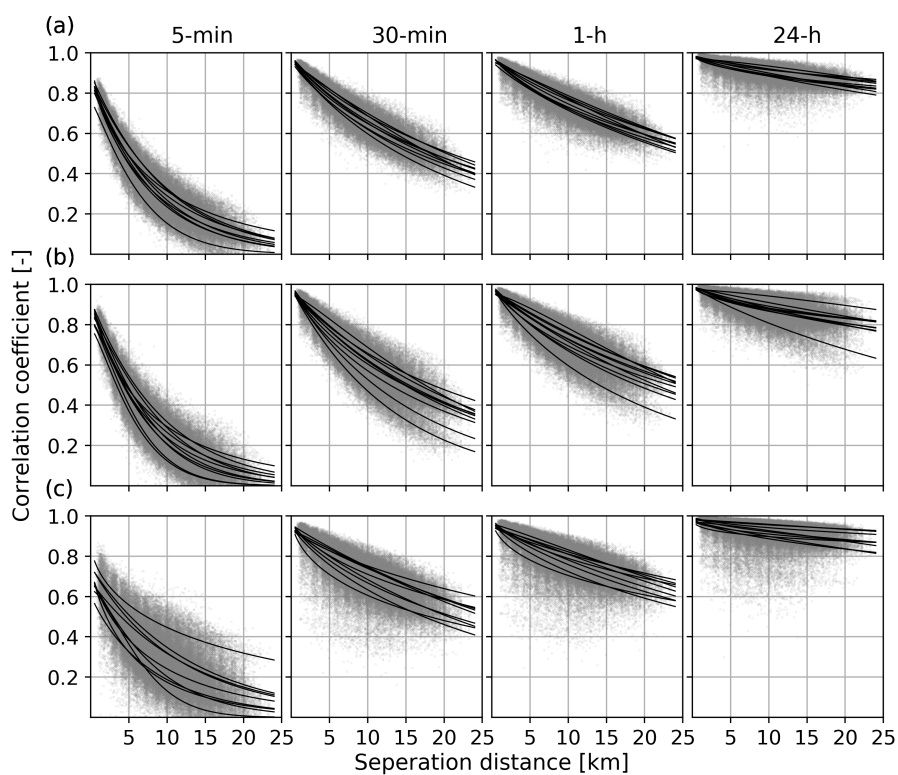


Figure 3. Spatial correlation of rainfall among rain gauges for (a) all-months, (b) wet season, and (c) dry season. Four selected accumulation times are shown. Each solid line represents a fitted exponential function for each year.

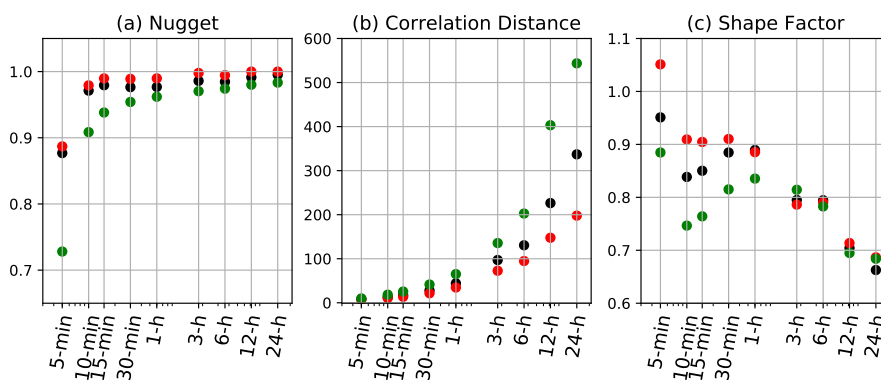


Figure 4. Dependence of (a) nugget, (b) correlation distance, and (c) shape factor of the fitted exponential functions on timescale (red: wet season, green: dry season, black: all-months).

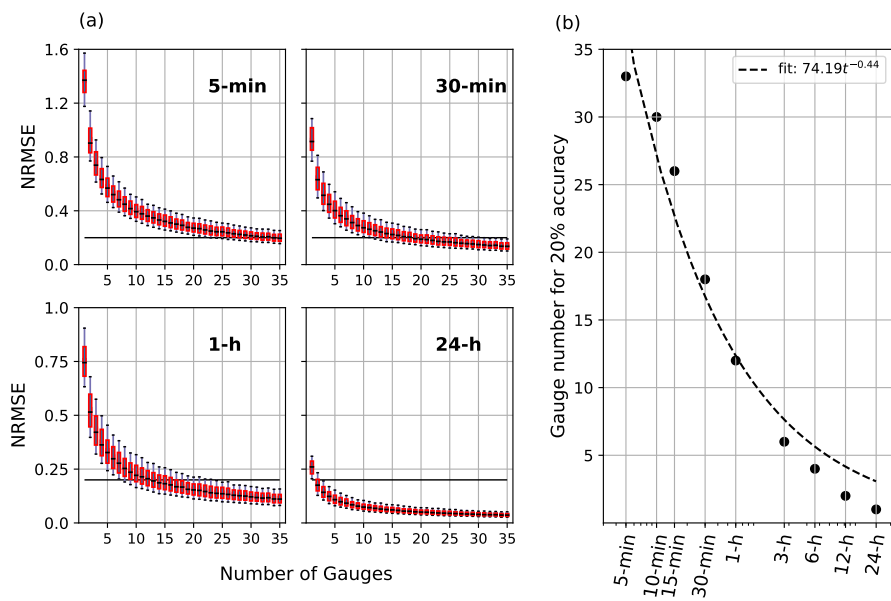


Figure 5. Dependence of the accuracy of areal rainfall estimates on the number of gauges during heavy rainfall. (a) Four selected time accumulations are shown. (b) The number of gauges required to obtain areal rainfall estimates with an normalized RMSE < 20%.

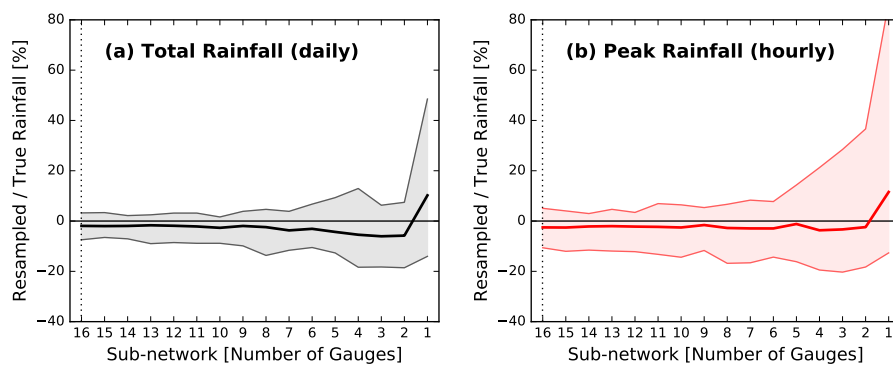


Figure 6. Dependence of the accuracy of (a) daily rainfall and (b) hourly peak intensity on the number of gauges. 71 heavy rain events are considered. The y axis displays the ratio of resampled rainfall to true rainfall. Resampled rainfall is calculated from n -gauge sub-networks, while true rainfall is calculated using the full density WEGN network.

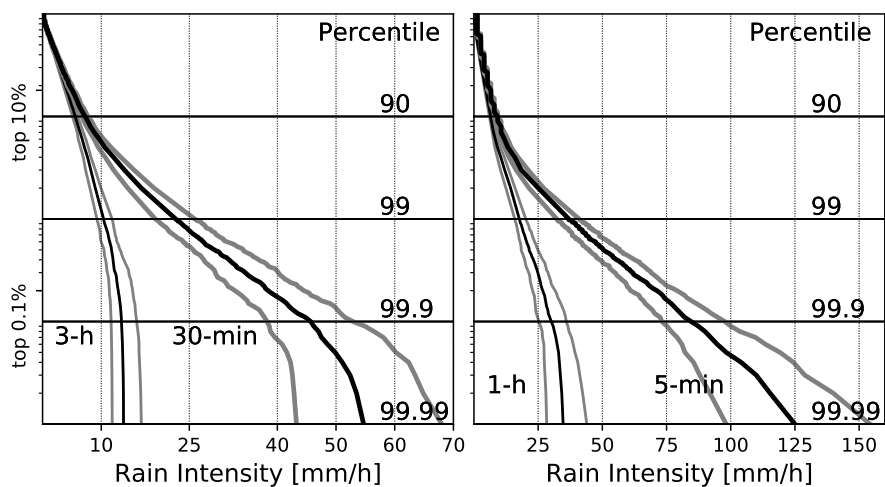


Figure 7. Distribution of gauge-level rainfall intensities corresponding to given percentile thresholds during heavy rainfall events. Four time scales are selected. Black lines show median values, gray lines show a 10th-90th percentile range among the gauges at a given threshold bin.

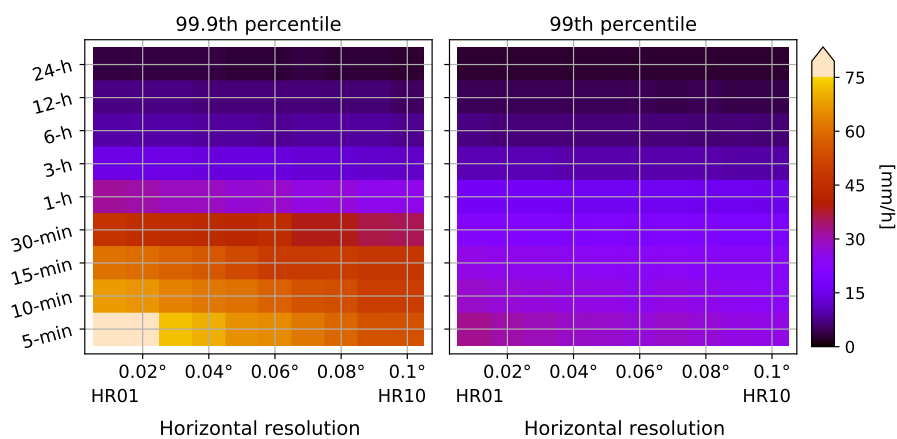


Figure 8. 99.9th and 99th percentiles of rainfall intensities derived from gridded rainfall fields with different spatial and temporal scales.

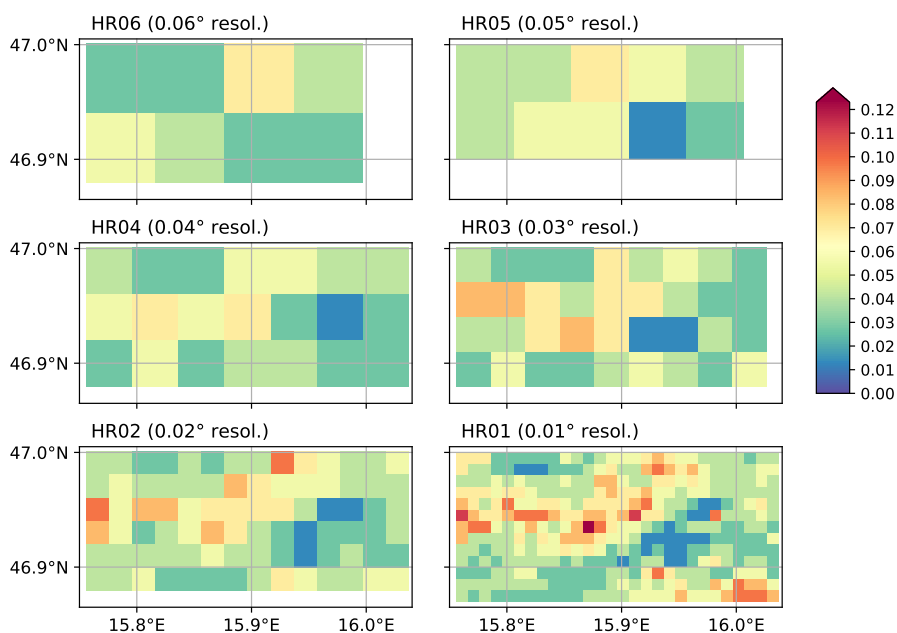


Figure 9. Occurrence of extreme events (≥ 95 th percentile of rainfall intensity during heavy rainfall events at HR01) at different horizontal grid spacing.

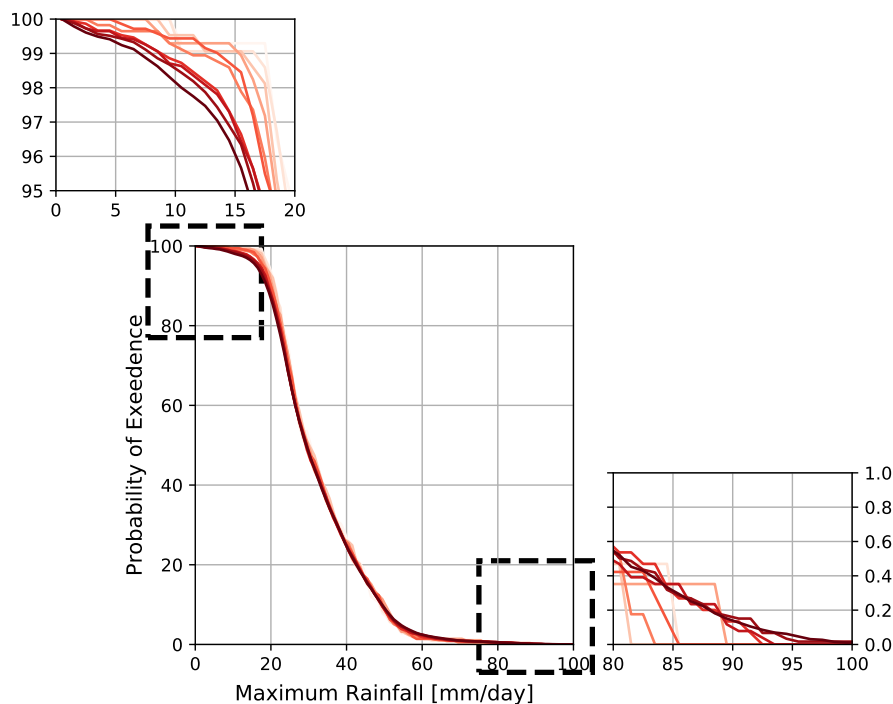


Figure 10. Probability of occurrence of heavy rainfall for different horizontal resolutions. Darker red represents higher horizontal resolution (from 0.1° to 0.01°).

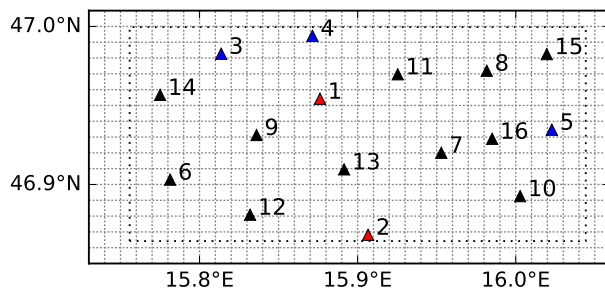


Figure A1. Selected WEGN gauges for Fig. 6. The gauges nearest to operational weather stations of the ZAMG and AHYD are in red and blue, respectively.